Slow Doping Rate in DNA−Poly(*o*-methoxyaniline) Hybrid: Uncoiling of Poly(*o*-methoxyaniline) Chain on DNA Template

Arnab Dawn and Arun K. Nandi*

Polymer Science Unit, Indian Association for the Cultivation of Science, Jadavpur, Kolkata-700 032, India

Received July 7, 2005; Revised Manuscript Received September 19, 2005

ABSTRACT: The doping rate of biomolecular hybrids of the deoxyribonucleic acid−poly(*o*-methoxyaniline) (DNA−POMA) system has been measured by UV−vis spectroscopy and pH study for the three different compositions (W_{DNA} = 0.21, 0.45, and 0.71, W_{DNA} = weight fraction of DNA) of the blend. Here the doping rate is very slow. The pH of the medium after an initial hike from 3.76 increases slowly with time and then levels up at around 5.75 in about 6 h. The UV−vis spectra of the hybrid solutions also exhibit a slow red shift of the π band−polaron band transition with time, and it levels up after 48 h of aging at 30 °C. Three stages of doping, e.g., (i) primary doping by phosporic acid group of DNA, (ii) uncoiling of POMA followed by doping, and (iii) slow uncoiling of POMA on DNA surface, are suggested for explaining the above behavior. The doping behavior has been studied at different isothermal temperatures, and Arrhenius analysis of the doping rate measured from the red shift of the π band−polaron band transition peak results in activation energy values ∼14 kcal/mol. This value is close to that of conformational transition of other polymers, supporting that the uncoiling process is the cause for the slow red shift of the π band−polaron band transition with time. The confinement of the POMA chain on the DNA surface catalyzes the uncoiling of POMA chain due to the cooperative repulsive interaction of the neighboring radical cations generated from the primary doping process. The conductivity values of the blend vary from 10^{-6} to 10^{-7} S/cm, and the $I-V$ curves characterize the hybrids as semiconductors.

Introduction

After the discovery of conducting polymer by MacDiarmid, Shirakawa, and Heeger,[1] a new era of biocommunication system is rapidly developing.[2−11] This is because the conducting polymers are electroactive polymers which reversibly switch between different oxidation states, releasing or uptaking different anions including biochemicals. The immobilization of deoxyribonucleic acid (DNA) on the conducting polymers is of great interest for its applications in DNA hybridization,[4] gene therapy,[3] and various biosensing applications.[12] Recently, poly(*o*-methoxyaniline) (POMA) in emeraldine base (EB) form has been used to make a biomolecular hybrid where the conformation of DNA and crystal structure of DNA remain unchanged.[7] Both DNA and POMA have very low conductivity, $\leq 10^{-13}$ S/cm, but the hybrid shows conductivity (10^{-7} S/cm) in the semiconducting region. The phosphoric acid groups of DNA dope POMA well, and the conductivity has been attributed for the doped POMA; DNA remained as a nonconducting component in the hybrid. It was observed that the doping process was very slow, and in this paper we want to shed light on the slowness of the doping process.

In the doping of POMA by DNA, transfer of proton from phosphoric acid group of DNA occurs to the nitrogen atom of POMA, resulting in the formation of radical cations (Scheme 1). In the doping medium (aqueous) the particle sizes of POMA, DNA, and POMA−DNA complexes are 668, 715, and 1353 nm, respectively (measured from the dynamic light scattering method), indicating that they are in colloidal range. The doping of colloidal POMA by phosphoric acid was instantaneous because of small size of the phosphoric acid molecule. So the colloidal nature of DNA has been attributed to the cause for the slowness of doping process.[7] Three probable reasons attributed for the slowness of doping behavior are (i) steric hindrance of DNA colloid to the POMA colloid, (ii) orientation of rigid DNA chain before interaction, and (iii) orientation of POMA chain during the process. As the DNA conformation and crystal structure remain unchanged during the doping process, so reason (ii) may be neglected, and in this paper we shall focus our attention on the other two factors.

Scheme 1

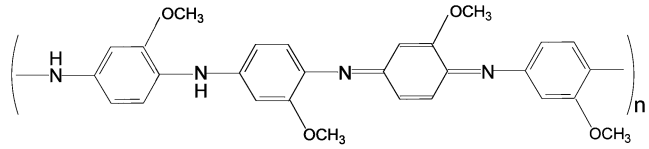

Poly (o-methoxyaniline) (Emeraldine base form)

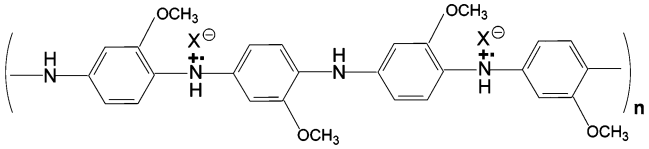

Poly (o-methoxyaniline) (Emeraldine salt form)

X^- is the DNA Anion

To get a complete idea of the doping process, it is needed to study the blends at different compositions. In this paper we made two different blends of compositions W_{DNA} = 0.21 and 0.71, apart from the earlier studied composition W_{DNA} = 0.45.[7] The pH of the POMA−DNA mixture is measured with time to get an idea of the doping behavior by proton transfer from phosphoric acid group of DNA. The temperature dependency of the doping behavior has been studied by UV−vis spectroscopy to understand the slow behavior of the

* Corresponding author. E-mail: psuakn@mahendra.iacs.res.in.

10.1021/ma051474r CCC: $30.25
Published on Web 11/02/2005

doping process that may occur from any physical phenomena. The morphology and the conductivity of the two new blends are also reported here as both may be affected in the doping process.

Both biopolymers and synthetic polymers undergo conformational transition with temperature in solution usually referred as helix−coil transition[13−19] or coil-to-order conformer transition.[20−22] Various investigations of helix−coil transition of synthetic polymers are made to study the effect of solvent composition,[18] counterion diffusion,[19] chain architecture,[15−17] etc. The coil to ordered ($TGT\bar{G}$) conformer transition during the gelation process was studied from the solution of PVF_2[21,22] by the test tube tilting method, and the transformation of coil to a order conformer of poly(3-hexylthiophene) was made by UV−vis spectroscopy.[20,23] In all these cases the conformational change is studied in solution state, but in the present work the situation is slightly different due to the colloidal nature of DNA. This is because during the initial doping process POMA may get absorbed on the DNA surface due to electrostatic interaction of the radical cation of POMA and the DNA anion.[7] Apparently, both POMA and DNA are in a common medium, but due to the absorption of the former on the DNA surface, if any conformational change of POMA occurs it may result in DNA templated conformational transition of POMA. In this paper an investigation of such type of conformational changes has been worked out from time-dependent pH and UV−vis spectroscopic studies. A kinetic analysis of the red shift of the π band to polaron band transition of doped POMA yielded activation energy values close to that of common polymers. This result supports that not only the DNA is doping POMA but also its surface is catalyzing the conformational transition of POMA, yielding a slow red shift of the π band to polaron band transition.

Experimental Section

Samples. Calf thymus DNA was purchased from Sigma Chemicals (type 1: sodium salt). The protonated form of DNA was prepared by mixing Na-DNA solution (0.02% w/v) and 0.01 N HCl solution followed by dialysis to remove sodium, chloride, and excess hydrogen ions.[7] POMA was synthesized in the laboratory from *o*-methoxyaniline in 1 M HCl medium in the presence of 5.8 M LiCl using ammonium peroxydisulfate.[7] Reactants in the molar ratio of 1.0:4.3:39.6 for ammonium peroxydisulfate, *o*-methoxyaniline, and 1.0 M HCl, respectively, were mixed at −35 °C, and the reaction mixture was stirred at −18 °C for 2 days. The polymer was collected by filtration and washed repeatedly with double distilled water. The emeraldine (EB) base form of POMA was made by stirring it with 0.1 M ammonium hydroxide solution for 48 h and then dried in a vacuum. The viscosity average molecular weight was found to be 20 900.[7] Sterilized double distilled water was used in all the work.

Preparation of the Hybrids. Aqueous solution of POMA (EB) (0.005% w/v) was made by sonication in an ultrasonic bath (60 W, model AVIOC, Eyela) for half an hour. A transparent blue solution was obtained. The protonated DNA solution (0.016% w/v) was then mixed in different proportions by volume with POMA solution (0.005% w/v) to make the hybrids of different compositions. The resultant solution was left undisturbed for a week at 30 °C and was then frozen dried to obtain the hybrid in the solid state.

Kinetics of Doping. To study the doping process, UV−vis spectra were performed in aqueous solutions of the DNA−POMA mixtures of different compositions in quartz cell of thickness 1 cm from 190 to 1100 nm using a Hewlett-Packard spectrophotometer (model 8453) at 30 °C. A pure water spectrum was taken as reference, and the UV−vis spectra were recorded at different aging times counted from the time of mixing. The experiment was repeated for solutions aged at different isothermal temperatures.

The doping process was also monitored from pH measurements of the POMA−DNA mixtures. The pH measurements of the solutions of different compositions were made using a pH meter (Denver Instruments, model 50) at 30 °C. The pH meter was standardized by standard buffer solutions of pH 4.0, 7.0, and 9.2. In the kinetic study the pH was monitored with time after the mixing of POMA and DNA solutions at room temperature (30 °C).

Characterization of the Hybrids. The scanning electron microscopy (SEM) was performed by drying one drop of aged (7 days) solutions of different compositions on a microscopic cover slide and finally dried in a vacuum at 30 °C for 2 days. It was then gold-coated and was observed in a SEM apparatus (Hitachi, S-2300).

The WAXS study of the hybrids was performed using a Philips X-ray diffractometer (PW 1830). Nickel-filtered Cu Kα radiation was used in the work. The samples were taken in the powder form, and the scan was made at the step size of 0.02° 2θ with 0.5 s per step.

The CD spectra of the aqueous solutions (aged for 7 days at 30 °C) of the hybrids were obtained using a spectropolarimeter (JASCO, J-600) in a 1 cm quartz cuvette.

The FT-IR spectra of the frozen-dried samples were studied in a Nicolet FT-IR instrument [Magna IR-750 spectrometer (series II)]. The hybrids were mixed with KBr, and pellets were made to run the scan. Subtraction of POMA spectra from the POMA−DNA spectra was done from the Omnic software installed in the instrument.

Dc Conductivity Measurement. The dc conductivities of the frozen -dried samples were measured at 30 °C by the two-probe method in a nitrogen atmosphere. The sample was sandwiched between two indium−titanium oxide (ITO) conducting strips of 1 mm width placed perpendicularly (area, $a = 1\ \text{mm}^2$), and the thickness (l) of the sample was measured using a screw gauge. The resistance of the sample was measured from a Keithley electrometer (model 617), and the conductivity was calculated from the relation

$$\sigma = \frac{1}{R}\frac{l}{a} \tag{1}$$

The $I-V$ characteristics of the samples were studied using the same samples by applying voltage from −1 to +1 V, and the current was measured at each applied voltage.

Results and Discussion

At first the physical characteristics of the blends will be discussed as this would assist to illuminate the complete doping mechanism of the systems.

Characterization of the Hybrids. In Figure 1 the scanning electron micrographs (SEM) of the hybrids are presented, and the micrographs are different from that of pure DNA having fibrillar network morphology.[7] The morphology of the DNA-rich hybrid is needlelike while that of the DNA-lean hybrid is of porous morphology. Such changes of morphology of the hybrids from that of pure DNA and also in the blends of different compositions support that mixing between DNA and POMA takes place, and the composition of the blend dictates the morphology. The CD spectra of the hybrid solutions are presented in Figure 2. It is apparent from the ellipticity vs wavelength plot that all the peaks of DNA are retained, signifying that DNA conformation does not change during the hybrid formation. The CD spectra also characterize the B-polymorphic structure of DNA in the hybrid.[24] The CD spectrum of POMA has an intense peak at 210 nm, and in the hybrids this peak is absent, indicating the occurrence of some conformational change of POMA in the hybrid.

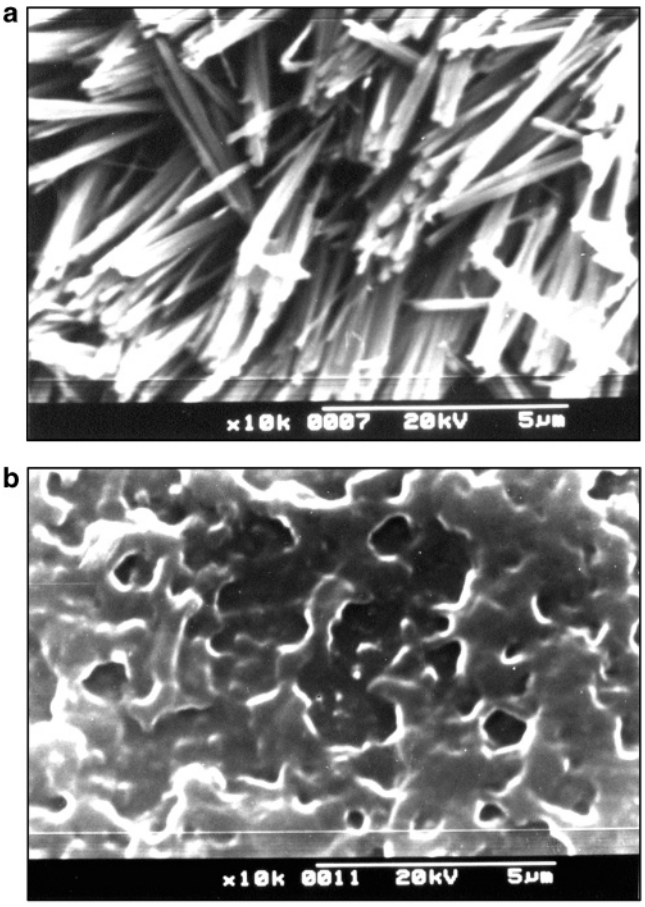

Figure 1. SEM micrographs of POMA−DNA hybrids: (a) $W_{DNA} = 0.71$ and (b) $W_{DNA} = 0.21$.

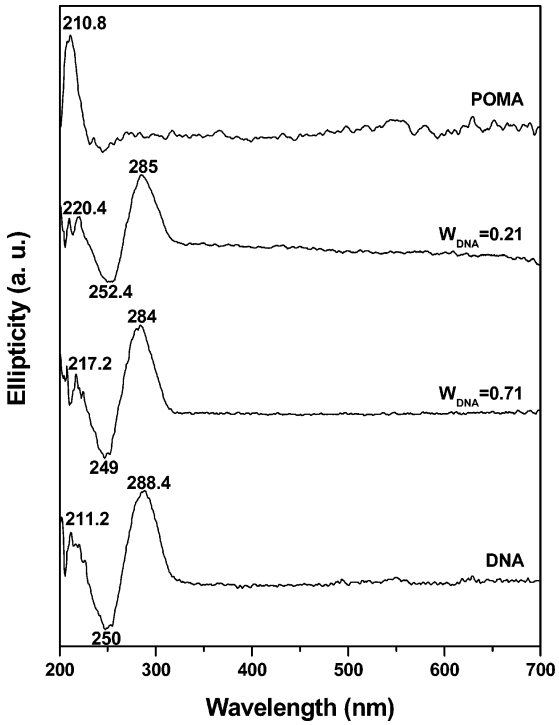

Figure 2. CD spectra of DNA, POMA−DNA ($W_{DNA} = 0.71$ and $W_{DNA} = 0.21$), and POMA (EB) solutions at 30 °C.

The WAXS patterns of Figure 3 clearly present that crystal structure of DNA remained intact as all the peaks of DNA are retained for the composition $W_{DNA} = 0.71$. However, the peaks of POMA are not observed in the blend, indicating POMA crystal structure might be lost. In the POMA-rich blend ($W_{DNA} = 0.21$) all the DNA peaks are not clearly observed because of dilution but the main peaks are clearly observed. The broadness of the amorphous peak in the hybrid is attributed to POMA as it has a broad amorphous peak. A careful look at the figure suggests that as POMA content decreases, the broadness also decreases and DNA peaks become more prominent. This indicates that the crystal structure of DNA is fully retained in the hybrid. Thus, it may be concluded that the conformation and crystal structure of DNA remain unaltered in the blends.

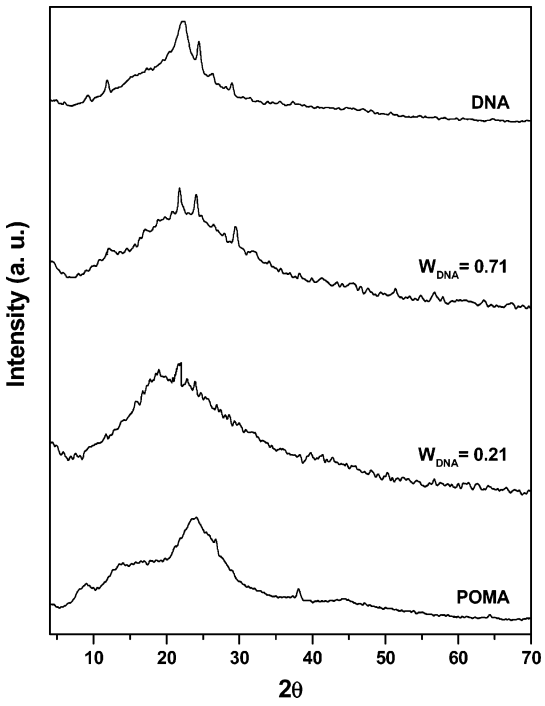

Figure 3. WAXS patterns of DNA, POMA−DNA hybrids ($W_{DNA} = 0.71$ and $W_{DNA} = 0.21$), and POMA (EB).

In the FT-IR spectra the 1701 cm^{-1} absorption peak for the deformation vibration of the O−H group of DNA[7,25] is absent in the blends, indicating that the phosphoric acid group of DNA is complexed with the nitrogen atom of POMA (Supplementary Figure 1). For the DNA-rich blend ($W_{DNA} = 0.71$) a small residual peak at ~1701 cm^{-1} is present characterizing that for the unreacted phosphoric acid group, indicating the presence of some residual DNA. Also from the UV−vis spectroscopy presented in the following section it would be evident that DNA is not denatured during the blending process. In a word such a mixing process yields the conducting polymer−DNA hybrid without affecting DNA conformation and structure.

Doping Behavior. The doping behavior of these systems has been studied from both UV−vis spectroscopy and pH study. Apart from the above studies at room temperature (30 °C) in the former method, the experiment was also performed at different isothermal temperatures.

UV−vis Study. In Figure 4 representative UV−vis spectra of the POMA−DNA system ($W_{DNA} = 0.21$) aged for different times at 30 °C are shown. From the figure it is apparent that the 599 nm peak of POMA (EB) characterizing the excitation of quinonoid ring[26−28] disappears, and a new peak at 655 nm showing a progressive red shift with increasing aging time appears. This new band is due to the transition of π band

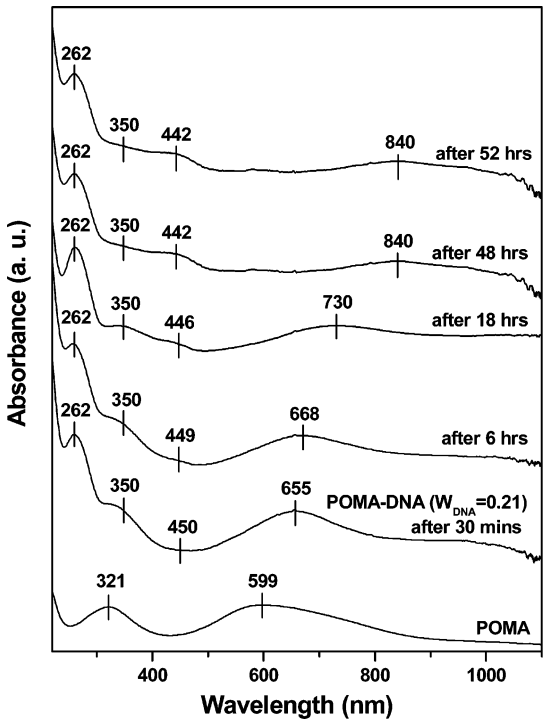

Figure 4. UV−vis spectra of POMA (EB) and POMA−DNA hybrid (W_{DNA} = 0.21) solution at indicated aging times at 30 °C.

to localized polaron band,[26−28] and it becomes invariant with time at 840 nm on 2 days of aging. The peak positions of the UV−vis spectra with aging time are given in Table 1. The 262 nm peak is for the DNA base pairs;[29] the 321 nm peak of POMA corresponds to a $\pi-\pi^*$ transition, and it shows a red shift when mixed with DNA. The peak at 450 nm arises from the polaron band to π^* band transition[26−28] and shows a blue shift with aging time. The most important observation is that in all the three samples red-shift of the π band to polaron band transition is a slow process and becomes fixed at 840−842 nm, irrespective of hybrid composition. However, the time for complete transition depends on the blend composition; the lower DNA content blend takes a longer time. This red shift of π band to localized polaron band transition with aging time causes the blue shift of the polaron band to π^* band.[26] A similar slow doping process is also observed in other compositions of the blend (Supplementary Figure 2); e.g., for the blend compositions W_{DNA} = 0.45 and 0.71 the constant absorption peak at ∼840 nm occurs at 30 h of aging at room temperature. The slowness of doping rate is more prominent with decrease in aging temperature. As for example for aging at 20 °C the doping is complete at 90, 77, and 72 h for blends of compositions W_{DNA} = 0.21, 0.45, and 0.71, respectively. In our earlier report for the blend of composition W_{DNA} = 0.45, it took about 15 days as the mixture was stored at 10 °C in the refrigerator. These results clearly suggest that there is a strong temperature dependency of the doping rate in the DNA−POMA hybrid.

pH Study. In Figure 5 the pH of the mixture is plotted with aging time for the three compositions of POMA−DNA hybrid kept at 30 °C. It is apparent from the figure that there is a rise of pH with time, and after 6 h of aging the pH becomes leveled at a value ∼5.8. The initial pH for DNA solution is 3.76, and within half an hour of mixing of POMA solution the pH of the mixture increased to a different extent depending on the composition of the blend (Figure 5). The initial increase of pH after 30 min of mixing is 0.94, 1.1, and 1.34 for W_{DNA} = 0.71, 0.45, and 0.21, respectively. Such an increase in pH of the medium is due to the reaction of nitrogen atoms of POMA with protons of DNA. The time 30 min is required to mix the solutions well and to measure the pH. The interesting observation is that the pH of the medium increases slowly with time, and at about 6 h of aging, the maximum pH is attained in all the three systems. These maximum pH levels are slightly different in the three compositions of the hybrid. The reason for the slow increase of the pH with time may be attributed for the slow reaction of POMA colloid with protons of DNA colloid. But the doping of POMA colloid by proton is fast as observed earlier from the doping by identical strength phosphoric acid solution.[7] So the slowness may be due to the slow ionization of phosphoric acid group of DNA or slow uncoiling of POMA rendering the nitrogen atoms of POMA available for doping or both. As pH of the medium after initial mixing are lower than that of water (6.8) (cf. Figure 5), so the first cause (i.e., slow ionization of phosphoric acid of DNA) may be neglected. Therefore, the slow uncoiling of POMA chain (cf. following section) reveals nitrogen atoms of POMA chain to be free, and then the doping takes place by the protons of DNA. The completeness of the primary doping process takes about 5−6 h, and then pH becomes constant at 5.7−5.9 depending on the DNA concentration. These lower pH values of the solutions than that of water (6.8) indicates slightly acidic nature of the medium. The slight difference in the pH value from that of water might arise from the unreacted phosphoric acid, ionization equilibrium of the POMA−DNA complex (salt of strong acid−weak base), etc.

Discussion

Now it is reasonable to understand the slowness of the doping process. From our earlier discussion on pH variation and the UV−vis spectra with time, it may be concluded that there are three steps in the doping process: (i) primary doping by the protons of DNA, (ii) uncoiling of POMA in the partially doped POMA followed by doping with DNA, and (iii) uncoiling of fully doped POMA leading to slow red shift of the π band to localized polaron band. Actually, it consists of two processes as the second process is a combination of uncoiling and primary doping. The reason for the slow uncoiling of POMA chain may be attributed for the confinement of doped POMA on the DNA surface through an electrostatic interaction of DNA anions and POMA radical cations generated during doping (Scheme 1). As the DNA conformation remains unchanged in the mixing process, it is reasonable to think that POMA molecules get absorbed on DNA surface, and the reverse is not true. Because of the surface confinement of POMA, the neighboring radical cations experience an electrostatic repulsion between themselves, causing the uncoiling of POMA chain. This uncoiling process increases the conjugation length, yielding the red shift of the π band to localized polaron band transition. To support this idea, we have made a temperature-dependent study of the doping process surrounding the room temperature such that any possibility of dedoping process at higher temperature is minimized. A representative figure showing the change in UV−vis spectra with doping temperatures for the same aging time

Table 1. UV−vis Peak Positions of POMA−DNA Hybrid at Different Blend Compositions for Different Aging Time at 30 °C

composition (W_{DNA})	aging time (h)	transition for base pair in DNA	$\pi-\pi^*$ transition (nm)	polaron band−π^* transition (nm)	π band−polaron band transition (nm)
0.21	0.5	262	350	450	655
	6	262	350	449	668
	18	262	350	446	730
	48	262	350	442	840
	52	262	350	442	840
0.45	0.5	262	351	447	667
	6	262	351	445	689
	18	262	351	443	801
	30	262	351	441	840
	35	262	351	441	840
0.71	0.5	262	352	446	668
	6	262	352	444	691
	18	262	352	442	807
	30	262	352	440	842
	35	262	352	440	842

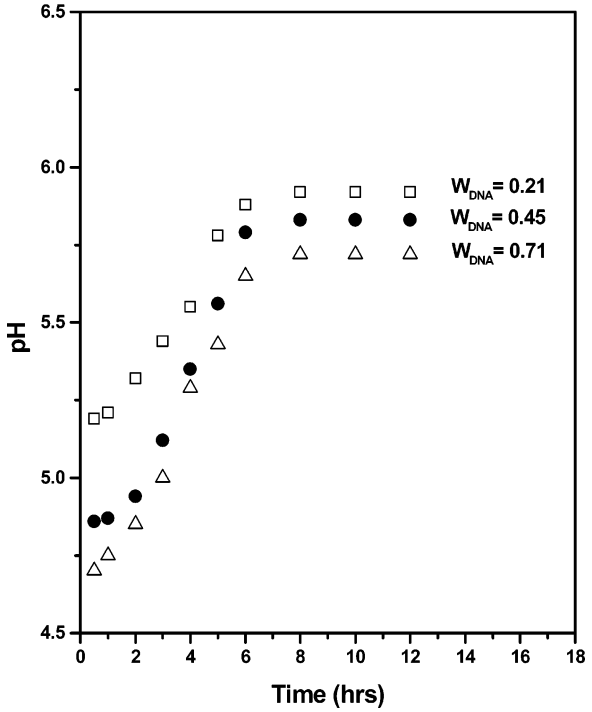

Figure 5. Variation of pH of POMA−DNA hybrid (W_{DNA} = 0.71, 0.45, and 0.21) solutions with aging time at 30 °C.

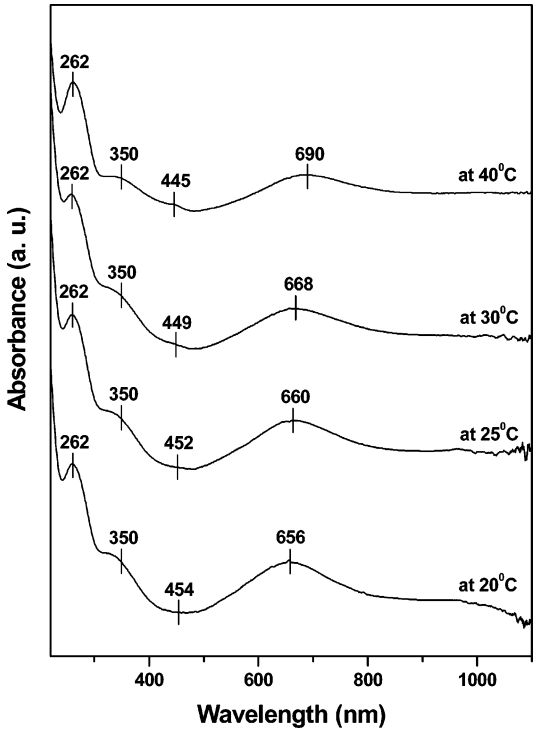

Figure 6. UV−vis spectra of POMA−DNA hybrid (W_{DNA} = 0.21) solution at indicated temperatures for 6 h of aging.

(6 h) is shown in Figure 6 for the blend $W_{DNA} = 0.21$. The figure clearly illustrates that there is a large shift of the π band to polaron band transition peak from 656 nm at 20 °C to 690 nm at 40 °C. This red shift may be attributed to the thermochromism at the same aging time (i.e., within same time frame), and it is also observed in other conducting polymers.[23,30,31] At the same aging time the red shift with temperature might occur for more uncoiling of POMA chain on the DNA surface due to the increased thermal motion of POMA chain. It should also be noted here that with increase in temperature there is blue shift in the polaron band to π^* band transition and may be attributed to the decrease of the π band to polaron band transition energy.[26] Similar behavior was observed in the other two compositions ($W_{DNA} = 0.45$ and $W_{DNA} = 0.71$) of the blend (Supplementary Figure 3a,b) where a gradual red shift of the π band to polaron band occurs with increasing temperature for the same aging time.

In Figure 7a−c the wavelength of the π band to polaron band transition is plotted with log of aging time at different isothermal temperatures for all the three compositions of the blend. At first there is a slow increase followed by a sudden rise, and finally there is leveling of the absorption peak position with log time. The sigmoidal behavior of the absorption peak position with log time is really interesting and represents an autocatalytic nature of the process. The initial slow increase of the π band to polaron band transition wavelength might be due to the slow uncoiling during the primary doping. As soon as the primary doping is over (~6 h, cf. Figure 5) uncoiling takes place very fast. This is evident from Figure 7 where the 30 °C isotherm shows the hike approximately at 6 h in the three compositions. However, with change in temperature there is some shift due to the temperature effect of the uncoiling process followed by doping. Probably complete confinement of POMA chain on the DNA surface catalyzes the uncoiling of the POMA chain due to the cooperative repulsive interaction of the radical cations of the complex. The repulsive force of the radical cations limits to the POMA chain only which resides on the DNA surface. It does not affect the inner base pairs of

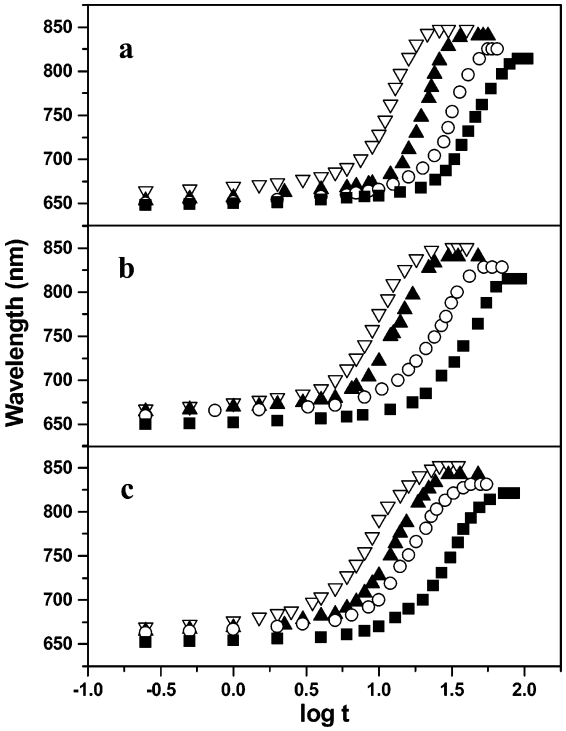

Figure 7. Wavelength of the π band to polaron band transition at 20 (■), 25 (○), 30 (▲), and 40 °C (▽) plotted against log t for POMA−DNA hybrid solutions: (a) $W_{DNA} = 0.21$, (b) $W_{DNA} = 0.45$, and (c) $W_{DNA} = 0.71$.

DNA, keeping its structure and conformation intact. The uncoiling of POMA chain when doped with smaller size acids like HCl, H_3PO_4, etc., might also be possible but the chain enlargement would not be stable because the counteranions are smaller in size and has rapid thermal movement. As a result, the interaction on doped POMA chain would fluctuate and would not exhibit any chain extension in the real term. On the other hand, the DNA anions being very large restrict the thermal movement and facilitate extension of POMA coil.[7]

To analyze the conformational transition of the uncoiling process, the Arrhenius equation of rate constant (k) may be used:

$$k = A\mathrm{e}^{-E/RT} \tag{2}$$

where A is the frequency factor, E is the activation energy of conformational transition for the uncoiling process, R is the gas constant, and T is the temperature of transition.

The rate constant of the conformational change k has been approximated as $1/\tau_{700}$,[20−22] where τ_{700} is the time required to reach the absorption maxima of the π band to localized polaron band at 700 nm in the UV−vis spectra of the samples.[32] Thus, a plot of $\ln(1/\tau_{700})$ against $1/T$ would be a straight line, giving negative slope with a value of E/R. In Figure 8 $\ln(1/\tau_{700})$ vs $1/T$ plots are shown, and straight lines are clearly obtained in all the cases. The correlation coefficient, least-squares slope, and least-squares intercept values are presented in Table 2. The correlation coefficient values certainly indicate that the straight line fitting of the data is good, indicating that the Arrhenius equation is applicable in the physical process presented here. Also, the intercept values are almost same for different blend compositions, suggesting almost the same value of frequency factor in the three hybrids. The activation energy of the

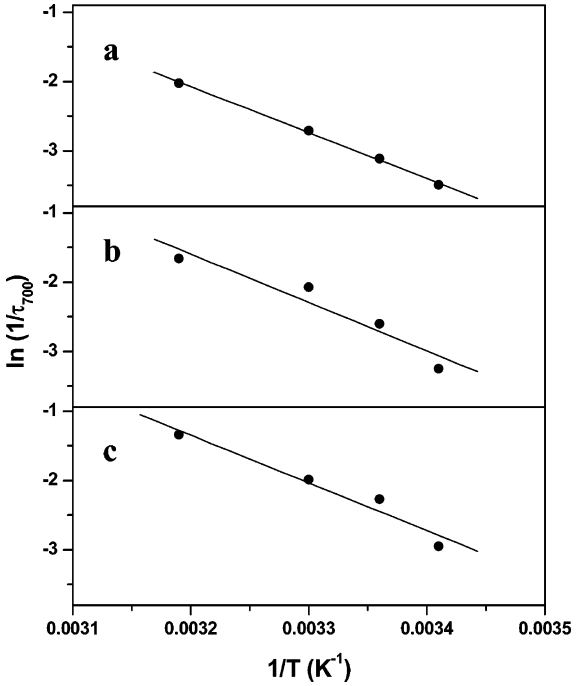

Figure 8. Arrhenius plot of $\ln(1/\tau_{700})$ vs $1/T$ for POMA−DNA hybrids: (a) $W_{DNA} = 0.21$, (b) $W_{DNA} = 0.45$, and (c) $W_{DNA} = 0.71$.

Table 2. Least-Squares Slope, Intercept, and Correlation Coefficient Values of Arrhenius Plots of POMA/DNA Hybrid Solutions at Different Blend Compositions

composition (W_{DNA})	slope (E/R)	intercept	correlation coefficient
0.21	6760	19.6	0.999
0.45	6985	20.7	0.968
0.71	6885	20.7	0.983

uncoiling process has been calculated from the least-squares slope value and is found to be 13.4, 13.9, and 13.7 kcal/mol for the hybrid of compositions (W_{DNA}) 0.21, 0.45, and 0.71, respectively. These activation energy values are close to the activation energy values for the conformational changes of conventional polymers. For example, Farmer et al.[33] calculated the energy difference between highest and lowest energy barrier of α polymorph of poly(vinylidene fluoride) (PVF_2) to be 9 kcal/mol; however, the activation energy of conformational transition measured from gelation kinetics of PVF_2 in diethyl adipate is ∼15 kcal/mol.[22] The theoretical value for the maximum energy change for the rotation of poly(3-hexylthiophene) (P3HT) with a change in dihedral angle from 0° to 90° is ∼15 kcal/mol.[34] However, the measured activation energy value from gelation kinetics of poly(3-hexylthiophene) in xylene is 23.7 kcal/mol.[20] So the present activation energy values obtained for the conformational transition of POMA are on the same order with those of other polymers. This supports that the red shift in UV spectra after primary doping is for the uncoiling of POMA on the DNA surface due to the conformational transition. As the DNA surface accommodates the POMA chain very well and assists the transition, it may be termed as DNA-templated conformational transition of POMA. This is a very new phenomenon of conformational transition of polymers on the DNA surface.

Conductivity. As doping of conducting polymers affects the conductivity so it should be discussed here. The dc conductivities of the hybrids at 30 °C are 1.18 ×

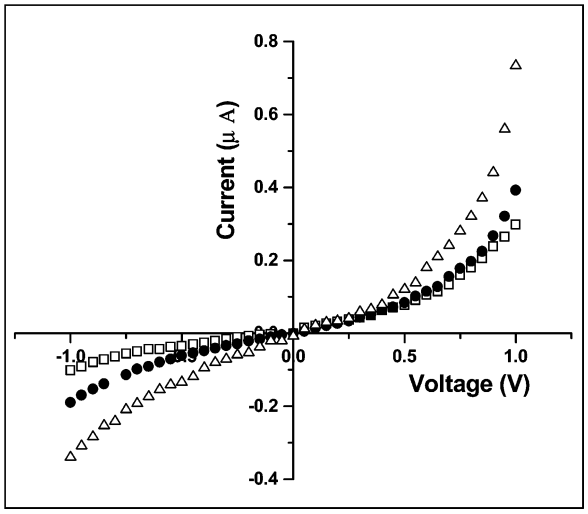

Figure 9. Current (*I*)−voltage (*V*) characteristic curves of POMA−DNA hybrids: $W_{DNA} = 0.21$ (□), $W_{DNA} = 0.45$ (●), and $W_{DNA} = 0.71$ (△).

10^{-7} and 2.88×10^{-6} S/cm for the hybrids of composition $W_{DNA} = 0.21$ and 0.75, respectively. The conductivity of 1:1 hybrid ($W_{DNA} = 0.45$) has a reported value of 9.73×10^{-8} S/cm while that of DNA is 5.23×10^{-13} S/cm. POMA (EB) is nonconducting and has value $<10^{-13}$ S/cm.[7] So in all the hybrids the conductivity is higher than that of the components. This increased conductivity is due to the doping of POMA (EB) by the phosphoric acid group of DNA. Here the POMA (emeraldine salt, ES) constitutes the percolating path, and DNA is present as a nonconducting material.[7] In Figure 9 the current (*I*)−voltage (*V*) characteristics of the biomolecular hybrids are presented, and the *I*−*V* curves represent the characteristics of semiconducting behavior.[35,36] So it may be concluded from these results that the POMA−DNA hybrids behave as semiconductors having conductivity in the 10^{-7}−10^{-6} S/cm region. A comparison of conductivity values clearly indicates the DNA-rich blend has 1 order higher conductivity than those of the other two blends where conductivity values are almost same. The reason for this increased conductivity is not yet clear, and a possible reason may be the higher doping level by the higher DNA concentration in the blend.

Conclusion

From this study it may be concluded that the doping of POMA by DNA consists of three processes: (i) primary doping, (ii) uncoiling of partially doped POMA followed by primary doping, and (iii) uncoiling of doped POMA. The first process is characterized by the sudden increase of pH and formation of the π band to polaron band; the second process is characterized by a slow increase in pH with time and also a slow red shift of the π band to polaron band transition. In the third process there is a sudden rise of the π band to polaron band peak with aging time due to the cooperative uncoiling process of absorbed POMA on DNA template. The activation energy of the uncoiling process was calculated to be ∼14 kcal/mol, characterizing the red shift is due to the conformational transition of POMA chain. The conductivity of the hybrids vary from 10^{-7} to 10^{-6} S/cm, approximately 6−7 orders higher than that of DNA. All the hybrids show *I*−*V* curves characteristic of a semiconductor.

Acknowledgment. We gratefully acknowledge the help extended by SINP, Kolkata, for X-ray study and Bose Institute, Kolkata, for CD measurements. A.D. also acknowledges the Council of Scientific and Industrial Research, New Delhi, for granting research fellowship.

Supporting Information Available: FT-IR spectra of POMA−DNA hybrids (Figure 1) and UV−vis spectra of POMA−DNA hybrids (Figures 2 and 3). This material is available free of charge via the Internet at http://pubs.acs.org.

References and Notes

(1) Shirakawa, H.; Louis, E. J.; MacDiarmid, A. G.; Chiang, C. K.; Heeger, A. J. *Chem. Commun.* **1977**, 578.
(2) Wallace, G. G.; Kane-Maguire, L. A. P. *Adv. Mater.* **2002**, *14*, 953.
(3) Wang, J.; Jiang, M. *Langmuir* **2000**, *16*, 2269.
(4) Thompson, L. A.; Kowalik, J.; Josowicz, M.; Janata, J. *J. Am. Chem. Soc.* **2003**, *125*, 324.
(5) Bae, A.-H.; Hatano, T.; Numata, M.; Takeuchi, M.; Shinkai, S. *Macromolecules* **2005**, *38*, 1609.
(6) Liu, B.; Bazan, G. C. *J. Am. Chem. Soc.* **2004**, *126*, 1942.
(7) Dawn, A.; Nandi, A. K. *Macromol. Biosci.* **2005**, *5*, 441.
(8) Gaylord, B. S.; Heeger, A. J.; Bazan, G. C. *J. Am. Chem. Soc.* **2003**, *125*, 896.
(9) Nagarajan, R.; Liu, W.; Kumar, J.; Tripathy, S. K.; Bruno, F. F.; Samuelson, L. A. *Macromolecules* **2001**, *34*, 3921.
(10) Lokshin, N. A.; Sergeyev, V. G.; Zezin, A. B.; Golubev, V. B.; Levon, K.; Kabanov, V. A. *Langmuir* **2003**, *19*, 7564.
(11) Saoudi, B.; Jammul, N.; Abel, M. L.; Chehimi, M. M.; Dodin, G. *Synth. Met.* **1997**, *87*, 97.
(12) Emr, S. A.; Yacynych, A. M. *Electroanalysis* **1995**, *7*, 913.
(13) Zimm, B. H.; Bragg, J. K. *J. Chem. Phys.* **1959**, *31*, 526.
(14) Flory, P. J.; Weaver, E. S. *J. Am. Chem. Soc.* **1960**, *82*, 4518.
(15) Buhot, A.; Halperin, A. *Europhys. Lett.* **2000**, *50*, 756.
(16) Buhot, A.; Halperin, A. *Macromolecules* **2002**, *35*, 3238.
(17) Kemp, J. P.; Chen, Z. Y. *Phys. Rev. Lett.* **1998**, *81*, 3880.
(18) Farago, O.; Pincus, P. *Eur. Phys. J.* **2002**, *7*, 393.
(19) Ciszkowska, M.; Osteryoung, J. G. *J. Am. Chem. Soc.* **1999**, *121*, 1617.
(20) Malik, S.; Jana, T.; Nandi, A. K. *Macromolecules* **2001**, *34*, 275.
(21) Mal, S.; Nandi, A. K. *Polymer* **1998**, *39*, 6301.
(22) Dikshit, A. K.; Nandi, A. K. *Macromolecules* **1998**, *31*, 8886.
(23) Rughooputh, S. D. D. V.; Hotta, S.; Heeger, A. J.; Wudl, F. *J. Polym. Sci., Part B: Polym. Phys.* **1987**, *25*, 1071.
(24) Sprecher, C. A.; Basse, W. A.; Johnson, W. C. *Biopolymers* **1979**, *18*, 1009.
(25) Colthup, N. B.; Daly, L. H.; Wiberley, S. E. *Introduction to Infrared and Raman Spectroscopy*; Academic Press: New York, 1964; p 300.
(26) Xia, Y.; Wiesinger, J. M.; MacDiarmid, A. G.; Epstein, A. J. *Chem. Mater.* **1995**, *7*, 443.
(27) Ruokolainen, J.; Eerikainen, H.; Torkkeli, M.; Serimaa, R.; Jussila, M.; Ikkala, O. *Macromolecules* **2000**, *33*, 9272.
(28) Stejskal, J.; Kratochvíl, P.; Radhakrishnan, N. *Synth. Met.* **1993** *61*, 225.
(29) Stryer, L. *Biochemistry*, 4th ed.; W.H. Freeman and Co.: New York, 1995; p 86.
(30) Faied, K.; Frechette, M.; Ranger, M.; Mazerolle, L.; Levesqu, I.; Leclerc, M.; Chen, T.-A.; Rieke, R. D. *Chem. Mater.* **1995**, *7*, 1390.
(31) Yang, C.; Orfino, F. P.; Holdcroft, S. *Macromolecules* **1996**, *29*, 6510.
(32) At the time required to reach the absorption maximum at λ = 700 nm only the cooperative uncoiling process due to the repulsion of neighboring radical cation starts for all the cases, and usually reaction rates are measured at initial transformation, so $1/\tau_{700}$ has been approximated as rate constant k.
(33) Farmer, B. L.; Hopfinger, A. J.; Lando, J. B. *J. Appl. Phys.* **1972**, *43*, 4293.
(34) Shibaev, P. V.; Schaumburg, T.; Norgaard, B. K. *Synth. Met.* **1998**, *97*, 97.
(35) Wu, C.-G.; Chang, S.-S. *J. Phys. Chem. B* **2005**, *109*, 825.
(36) Lee, H. J.; Park, S.-M. *J. Phys. Chem. B* **2004**, *108*, 1590.

MA051474R